Supporting Information for

# Topotactic N-doped carbon for efficient oxygen reduction reaction

Miaosen Yang[a], Tian Zhang[a,b], Danni Wang[b], Yingna Chang[c], and Guoxin Zhang[b,*]

a. School of Chemical Engineering, Northeast Electric Power University, Jilin, Jilin 132012, China.

b. College of Energy Storage Technology, Shandong University of Science and Technology, Qingdao, Shandong 266590, China. Email: zhanggx@sdust.edu.cn

c. Institute of New Energy on Chemical Storage and Power Sources, College of Applied Chemistry and Environmental Engineering, Yancheng Teachers University, Yancheng 224000, China.

## 1. Experimental Section

*2.1 Chemicals and materials:* Polyvinyldichloride (PVDC, DiofanÂ® P 530, Solvay Specialty Polymers) was purchased from Changzhou Mingshuo Chemical Co., Ltd. Other reagents, carbon nanotube (CNT, purity＞99%, used without treatment) was purchased from Shenzhen Suiheng Technology Co., Ltd. Sodium ethoxide ($C_2H_5ONa$, A.R. grade), N-Methyl pyrrolidone (NMP, A.R. grade), pyridine (A.R. grade), pyrrole (A.R. grade), melamine (A.R. grade) were all purchased from Shanghai Macklin Bio-chemical Co., Ltd.

### *2.2 Material characterizations*

X-ray diffraction (XRD) patterns were recorded by a Shimadzu XRD-6000 (CuKα radiation, $\lambda$= 1.5406 Å, 40 kV) in the $2\theta$ range of 5-80˚. Raman spectroscopy was obtained from LabRAM ARAMIS Raman spectrometer (HORIBA Jobin Yvon). Scanning electron microscopy (SEM) images were measured on an Apreo S Hivac scanning electron microscope with an accelerating voltage of 20 kV. Transmission electron microscopy (TEM) and high-angle annular-dark-field scanning transmission electron microscopy (HAADF-STEM) images were obtained on an FEI Talos 200S high-resolution transmission electron microscope at an accelerating voltage of 200 kV. X-ray photoelectron spectroscopy (XPS) data were obtained with a Thermo ESCALAB 250Xi spectrometer. The specific surface area and pore structures of the N-doped carbons were studied by the $N_2$ adsorption-desorption isotherm (Micromeritics ASAP 2460) using a Micromeritics ASAP 2460 instrument at 77 K.

### *2.3 Electrochemical measurements of the oxygen reduction reaction*

The ORR catalytic activity of the N-doped carbon samples is evaluated in a three-electrode setup connecting to an electrochemical workstation (CHI-760E), a Pt wire and a saturated calomel electrode (SCE) are used as the counter and reference electrodes, respectively, and a glass carbon electrode loaded with catalyst ink is used as the working electrode. The catalyst ink is prepared as follows: 5.0 mg of catalyst and 1.0 mg of conductive carbon black are homogeneously dispersed in 30 μL of Nafion (0.5 wt %) and 970 μL of ethanol solution to form a uniform slurry. Before the ORR test, $O_2$ (99.999%) is purged into 0.1 M KOH electrolyte for at least 30 min to reach $O_2$ saturation. Commercial Pt/C (20 wt%) was used as a standard catalyst for ORR testing. According to the Nernst equation, all potentials are converted to reversible hydrogen electrode (RHE):

$$E_{RHE} = E_{SCE} + 0.059\ V \times pH + 0.241\ V \tag{1}$$

where $E_{RHE}$ is the potential relative to RHE, and $E_{SCE}$ is the measured potential relative to the SCE reference electrode. To investigate the ORR kinetics, the linear sweep voltammetry (LSV) curves are measured in $O_2$-saturated 0.1 M KOH with a scan rate of 5 mV $s^{-1}$ at different speeds ranging from 400 to 2025 rpm. Koutecky-Levich (K-L) plots are used to calculate the electron transfer number ($\boldsymbol{n}$):

$$\frac{1}{J} = \frac{1}{J_K} + \frac{1}{J_L} = \frac{1}{J_K} + \frac{1}{B\omega^{1/2}} \tag{2}$$

$$B = 0.62nFC_0D_0^{2/3}v^{-1/6} \tag{3}$$

where the J, $J_L$, and $J_K$ are the experimental measured current density, the diffusion-limiting current density, and the kinetic current density. Here, $\omega$ represents the rotating speed (in rpm), $n$ is the number of transferred electrons for ORR, F is the Faraday constant, $C_0$ is the bulk concentration ($1.2\times10^{-3}$ mol $L^{-1}$), $D_0$ is the diffusion coefficient of $O_2$ ($1.9\times10^{-5}$ $cm^{-2}$ $s^{-1}$), and $v$ is the kinetic viscosity (0.01 $cm^{-2}$ $s^{-1}$). The Tafel curves are obtained through the LSV polarization curves according to the following equation:

$$\eta = a + b\log|j| \tag{4}$$

## 2. Supplementary Figures

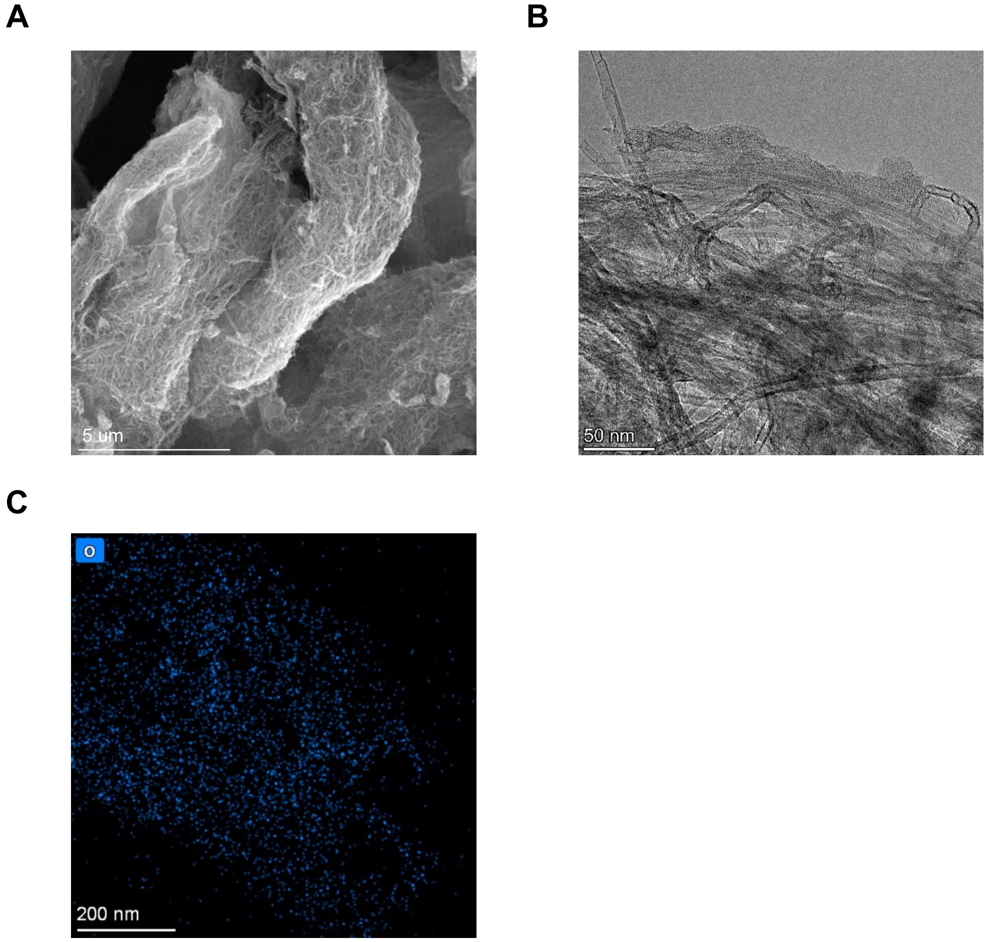

**Figure S1.** (A) SEM image, (B) TEM image, (C) oxygen element mapping image of $N_{pyri}$-C.

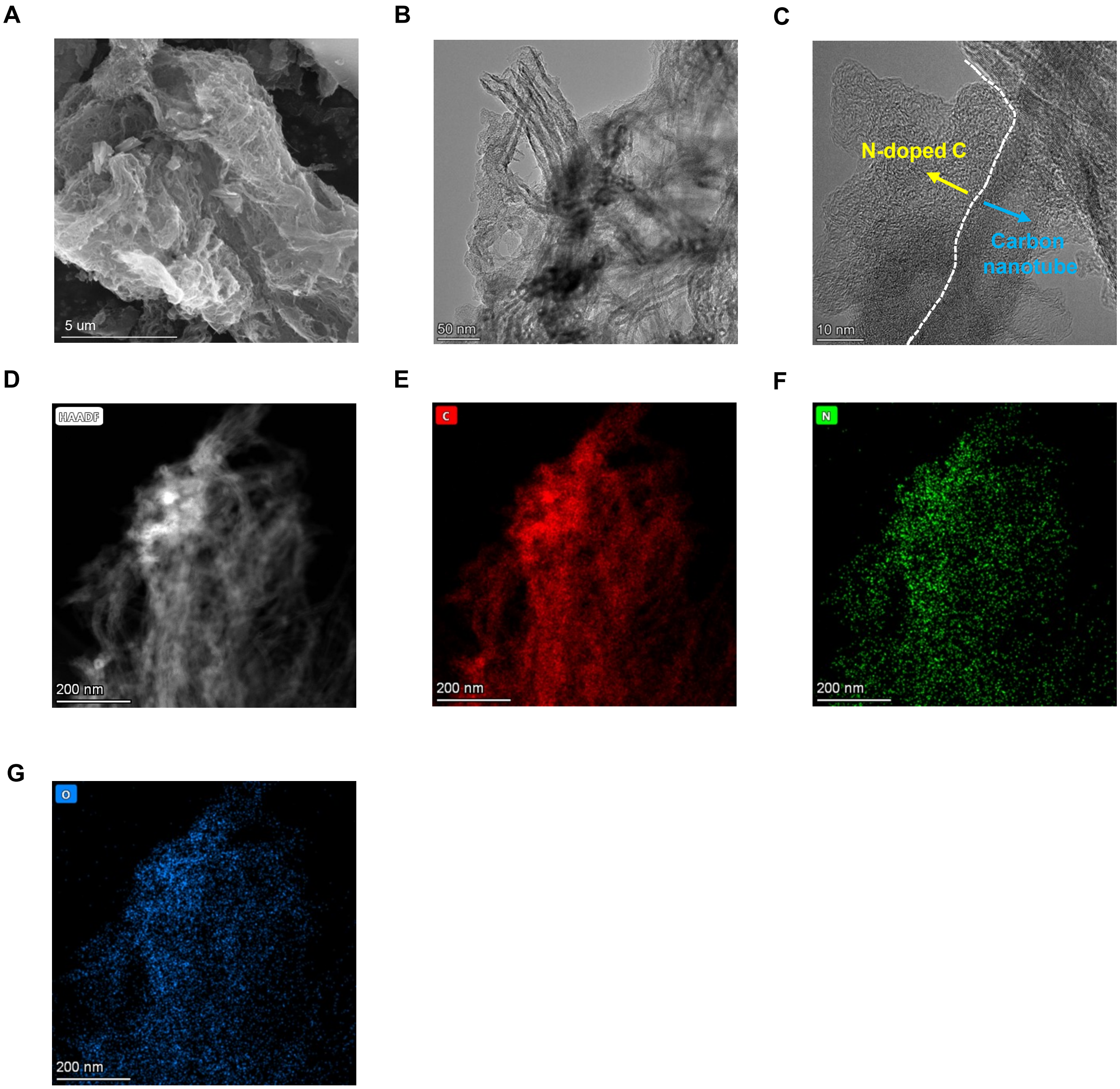

**Figure S2.** (A) SEM image, (B) TEM image, (C) HRTEM image, (D) HAADF-STEM image, (E) carbon, (F) nitrogen, and (G) oxygen element mapping images of $N_{pyrr}$-C.

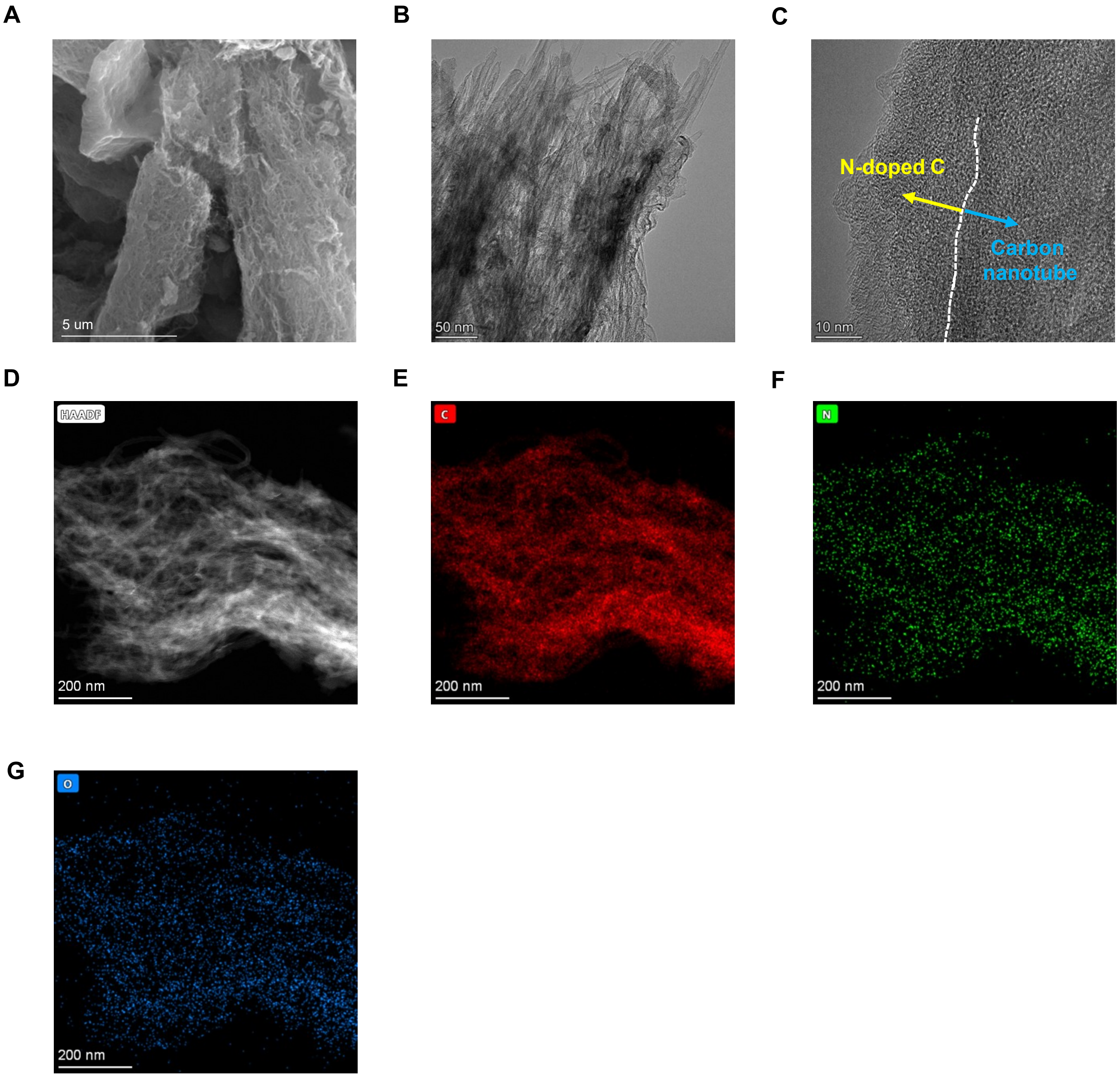

**Figure S3.** (A) SEM image, (B) TEM image, (C) HRTEM image, (D) HAADF-STEM image, (E) carbon, (F) nitrogen, and (G) oxygen element mapping images of $N_{NMP}$-C.

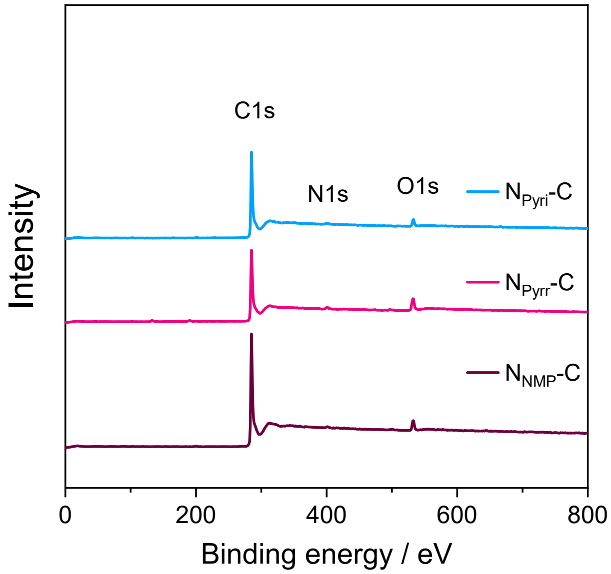

**Figure S4.** XPS survey spectra of $N_{pyri}$-C, $N_{pyrr}$-C, and $N_{NMP}$-C samples.

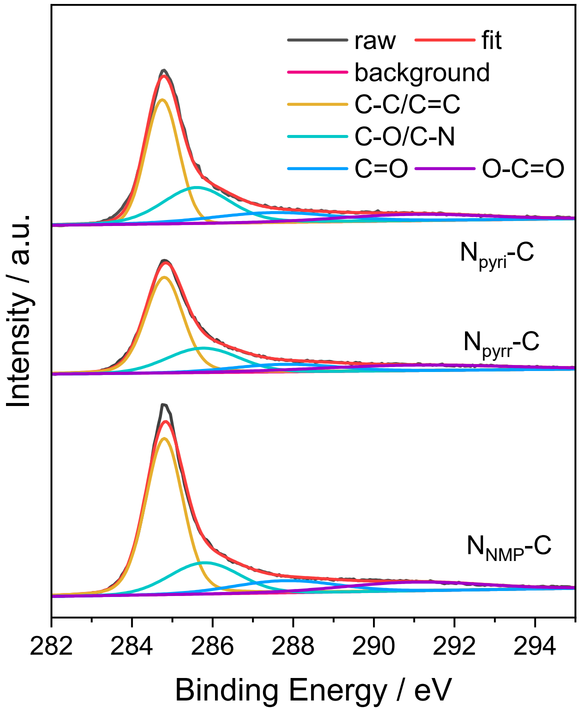

**Figure S5.** XPS C 1*s* spectra and the deconvoluted curves of $N_{pyri}$-C, $N_{pyrr}$-C, and $N_{NMP}$-C samples.

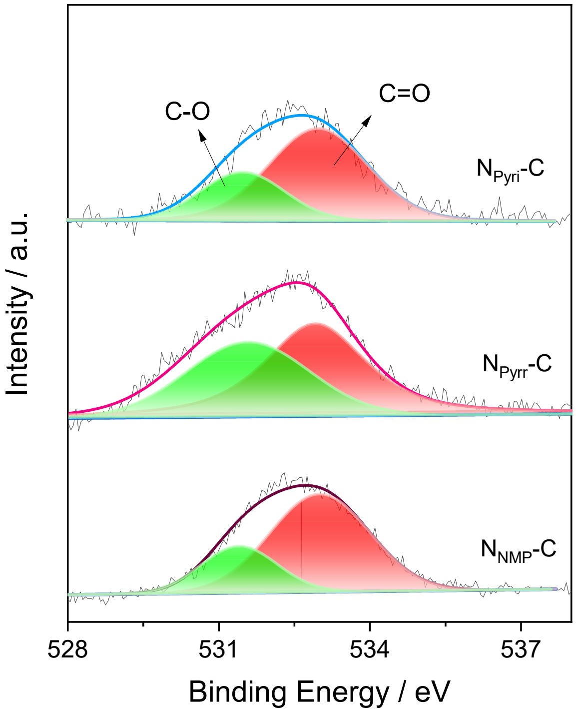

**Figure S6.** XPS O 1*s* spectra and the deconvoluted curves of $N_{pyri}$-C, $N_{pyrr}$-C, and $N_{NMP}$-C samples.

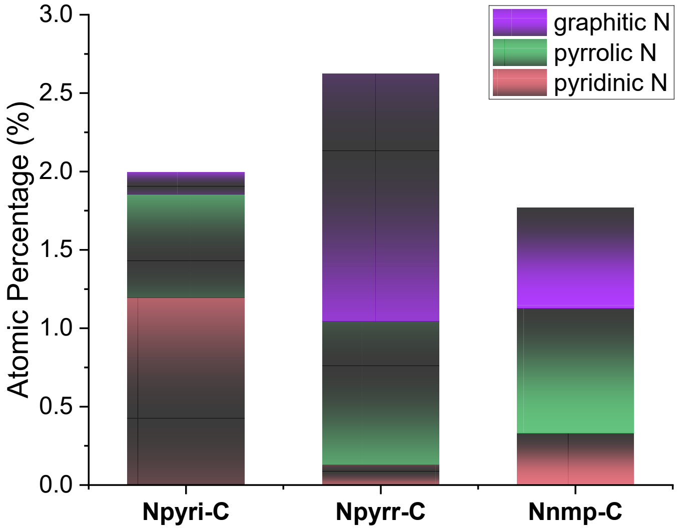

**Figure S7.** The actual atomic percentages of different types of N species in N-C/CNT composites based on XPS elemental analysis.

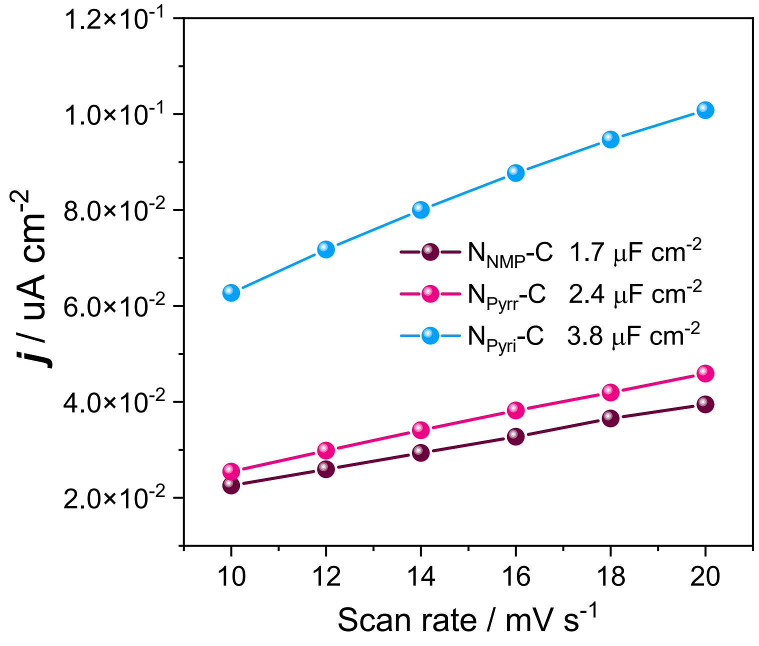

**Figure S8.** Plots of CV peak current density versus scan rate for $N_{pyri}$-C, $N_{pyrr}$-C, and $N_{NMP}$-C.

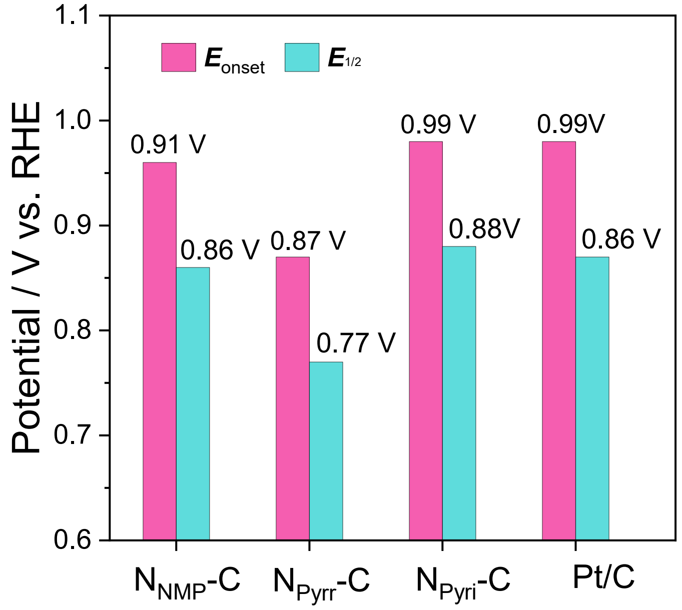

**Figure S9.** Comparisons of onset potential and half-wave potentials of $N_{pyri}$-C, $N_{pyrr}$-C, and $N_{NMP}$-C using 1600-rpm LSV polarization curves.

**Table S1.** Performance comparison of our N-doped carbon with other metal-free doped carbons reported.

| | Electrolyte | $E_{oneset}$ (V) | $E_{1/2}$ (V) | Tafel (mV dec$^{-1}$) | Durability (i-t method, retention@time duration) | Reference |
|---|---|---|---|---|---|---|
| $N_{Pyri-C}$ | 0.1 M KOH | 0.99 | 0.88 | 110.3 | / | This work |
| $N_{Pyrr-C}$ | | 0.87 | 0.77 | 101.7 | 98%@6h | |
| $N_{NMP-C}$ | | 0.91 | 0.86 | 89.4 | / | |
| NC-6 | 0.1 M KOH | 0.87 | 0.81 | / | 94%@4h | Nano-Micro Lett. (2018) 10: 29 |
| NPCS-900 | 0.1 M KOH | 0.99 | 0.87 | / | 16 mV $E_{1/2}$ loss after 5000 cycles | J. Mater. Chem. A, 2021, 9: 5751 |
| NDC1000 | 0.1 M KOH | 0.96 | 0.86 | / | / | Angew. Chem. 2020, 132(29): 12097 |
| NPCNF-O | 0.1 M KOH | 0.98 | 0.85 | 66 | 90%@6.9h | ACS Catal. 2022, 12(7): 4002 |
| N-CNSP | 0.1 M KOH | 0.96 | 0.85 | 58 | 95%@16.7h | Energy Storage Mater 2020, 27: 514 |
| NCF | 0.1 M KOH | 1.00 | 0.86 | 57 | 88.9%@24h | Adv. Funct. Mater. 2021, 31, 2103187 |